MAJOR QUALIFYING PROJECT

Worcester Polytechnic Institute

MIG-10 and UNC-53

Two proteins involved in neuron migration and excretory canal outgrowth

Sana Hashmi and Mark Kuhlwein

4/28/2011

MIG-10 and UNC-53:
Two proteins involved in neuron migration and excretory canal outgrowth

A Major Qualifying Project
submitted to the Faculty of
WORCESTER POLYTECHNIC INSTITUTE
in partial fulfillment of the requirements for the
degree of Bachelor of Science

by
Sana Hashmi and Mark Kuhlwein

Date:
Apr 28, 2011

Report Submitted to:

Professor Elizabeth Ryder
Worcester Polytechnic Institute

Table of Contents

Abstract

Mutations in *mig-10* and *unc-53* in *C. elegans* result in defects in axon guidance and excretory canal outgrowth. To better understand these genes' effects on migration and outgrowth, single and double mutant phenotypes were compared. In *mig*-10 mutants, excretory canal truncation is first observed during embryogenesis. Rescue experiments show that MIG-10 functions cell autonomously in the excretory cell. Phenotypes of single and double mutants suggest that *mig-10* and *unc-53* may have varying functions in different cells.

Acknowledgements

First and foremost, the two of us cannot give enough thanks to our adviser, Dr. Liz Ryder. Her presence as a teacher and adviser has constantly motivated us to excel during the course of this project and has provided us with the incentive to pursue the field in the future. In addition to the research and statistical skills she has imparted, we are grateful for the chance to work with her and learning so much more on both a professional and personal level. Secondly, we would like to thank Molly McShea, without whom the two of us would most likely be stumbling along the path of failure. She has been a joy to work alongside of, both as a friend and as a role model. In addition, we would like to thank Professor Sam Politz and the members of the Politz Lab for their presence, support, and of course, equipment use.

Introduction

Developmental neurobiology aims to understand the mechanisms behind the formation of the nervous system during embryonic development and throughout later growth. The network formed by the nervous system is essential for information processing (Tessier-Lavigne & Goodman, 1996). During development, neurons travel large distances along a path to their correct target in order to form the correct network necessary for neural circuits. Extracellular guidance cues are necessary for neurons to perform this function, as they respond to signals necessary for guiding axons along the pathway to their final location (Dickson, 2002). Miswiring of neural circuits can lead to a dysfunctional nervous system commonly associated with several developmental disorders such as Down's syndrome and autism as well as neurodegenerative disorders and nervous system injuries (Quinn & Wadsworth, 2008; Yaron & Zheng, 2008). Therefore, it is essential to understand the mechanisms responsible for guidance of the nervous system in order to develop means of repairing these disorders and injuries.

Neuronal and axonal migration studies have led to the identification of several factors that play a key role in the development of the system (Dickson, 2002). Guidance molecules and their corresponding surface receptors have been identified; however, the cytoplasmic mechanisms underlying the exact nature of the guidance process is still being understood (Yu & Bargmann, 2001). Therefore, understanding the genes and corresponding proteins involved in axon guidance is integral to the developing nervous system. In this project, the *C. elegans* proteins MIG-10 and UNC-53, which facilitate connections between guidance signals and cellular responses, are studies for their role in pathways associated with neuron migration and development.

Key Terms and Abbreviations

ALM Anterior Lateral Microtubule neuron

AVM Anterior Ventral Microtubule neuron

EC Excretory Canal

LPD lamellopodin

MIG abnormal cell MIGration

PLM Posterior Lateral Microtubule cell

PVM Posterior Ventral Microtubule cell

UNC UNCoordinated

Background

C. elegans as a model organism

As the first multicellular organism with its complete genome sequenced, the nematode *C. elegans* is well suited for genetic analysis due to its small size and rapid life cycle (Hodgkin, 2005). Its nervous system, which has been characterized extensively, is the nematode's most complex organ with the largest cellular diversity (Hobart, 2005). *C. elegans* is well suited for cell migration analysis due to the fact that cell movement and migrations are consistent among individuals(Manser et al., 1997).

Embryology

The rapid lifecycle of *C. elegans* allows it to act as a model organism in studying the development of the nervous system. Within its 3 day life cycle, the nematode passes through several distinct phases, each unique in terms of development and growth. Embryogenesis itself can be divided into several smaller phases, characterized by marker events and the number of nuclei present within the embryo (Sulston et al., 1983). This process can be divided into two phases of roughly equal duration: 1) cell proliferation and organogenesis, and 2) morphogenesis (Wood). During cell proliferation and organogenesis, cell divisions, cell movements, and death begin to occur, producing an embryo with approximately 550 cells roughly 7 hours after fertilization. The remaining 7 hours of embryo growth, known as morphogenesis, results in the outgrowth of neural processes as well as their interconnection. In addition, the embryo begins to elongate and move, resulting in growth of an organism that is almost three times the length of the egg just prior to hatching (Sulston et al., 1983). The L1 stage larva hatches at roughly 14 hours after fertilization, containing 558 cells within the hermaphrodite (Wood).

During morphogenesis, the embryo takes on several distinct shapes, identifiable via Differential Interface Contrast (DIC) optics (Figure 1). Morphogenesis of the embryo can take 2 hours maximum, demonstrating the growth and development of the egg, and is usually complete in terms of growth by 600 minutes. The remaining two hours of embryogenesis are dedicated to extraneous cell deaths, cuticle synthesis, and pharynx development (Sulston et al. 1983). Upon hatching, larval development progresses through four stages: L1, L2, L3, and L4 before the animal molts to an adult phase.

As the largest cell in *C. elegans*, the excretory cell is easily visible and serves as a landmark identifier in embryonic development (Sulston et al. 1983; Buechner, 2002). After its birth, the excretory cell extends two processes anteroposterially, creating an identifiable H-

shape. By the time the worm hatches, the posterior canals have reached half the length of the worm, and continue to extend throughout the L_1 stage. After the L1 stage, the excretory canals continue to grow passively with its length, matching the overall growth (Buechner, 2002).

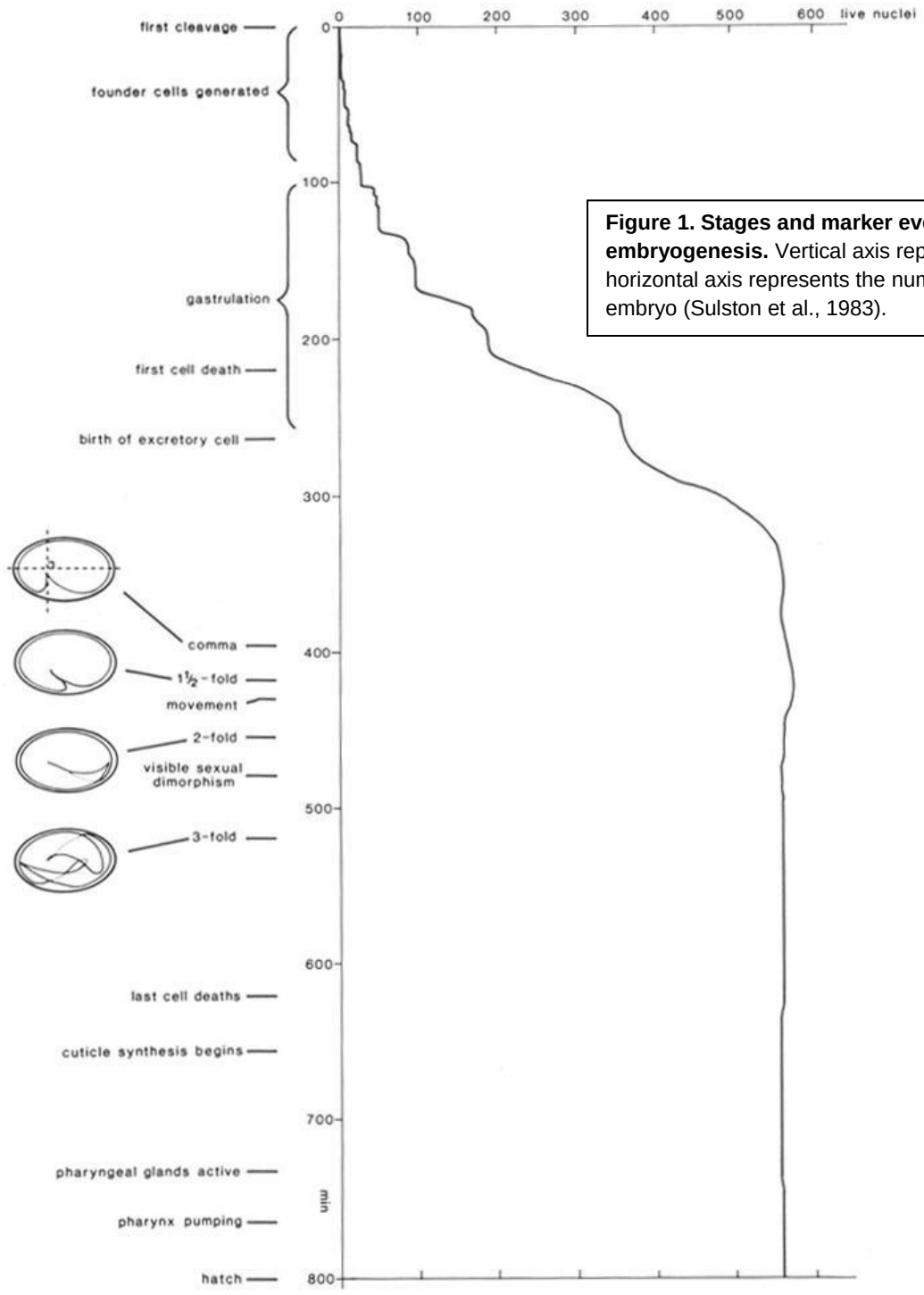

Figure 1. Stages and marker events during embryogenesis. Vertical axis represents time in minutes, horizontal axis represents the number of total cells in the embryo (Sulston et al., 1983).

Neuron Cell Body Migration

In the early stages of the *C. elegans* lifecycle, cells migrate to their final destinations. This act is accomplished by cells being attracted or repelled by certain cues. These cues can be Wnt proteins, which form anterior posterior gradients (Zou 2006), or other cues such as UNC-6 and SLT-1, which form dorsal ventral gradients (Quinn 2008). Migrating cells form a growth cone which detects these cues and initiates migration (Hedgecock 1987). Different cells, having varying receptors, respond differently to these cues, which act as either attractants or repellants.

Some of the mechanosensory neurons migrate long distances in the early stages of *C. elegans* as well (Figure 2). For example, during embryogenesis, the Anterior Lateral Microtubule (ALM) migrates posteriorly. The Anterior Ventral Microtubule (AVM) migrates anteriorly during the L1 larval stage.. Also during the L1 larval stage, the Posterior Ventral Microtubule (PVM) migrates first posteriorly and then has a second, anterior, migration (Hedgecock 1987). These mechanosensory neuron cell body migrations are truncated in *mig-10* mutant worms (Silhankova 2007). The Posterior Lateral Microtubule (PLM) has no known migration, though it does have a process which it sends anteriorly across the worm (worm atlas & Figure 2).

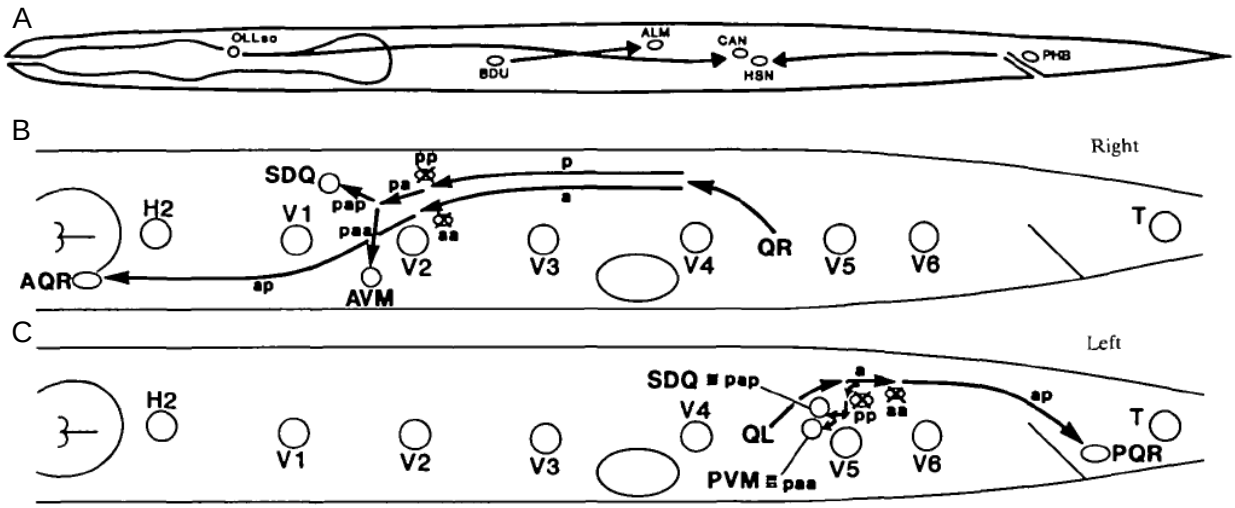

Figure 2: Migrations of the Mechanosensory Neurons. A) ALM Migration. Although this migration occurs during embryogenesis, it is shown superimposed on the larval L1 stage. B). AVM Migration. C) PVM Migration. (Hedgecock, 1987).

MIG-10: Cytoplasmic Adaptor Protein

The protein MIG-10 is the *C. elegans* member of the MRL family of cytoplasmic adaptor proteins. In addition to MIG-10, this family contains vertebrate proteins RIAM and Lamellopodin (Figure 3). Members of this family share conserved Ras association and pleckstrin homology domains. Furthermore, the MRL protein family also contains proline rich regions that are

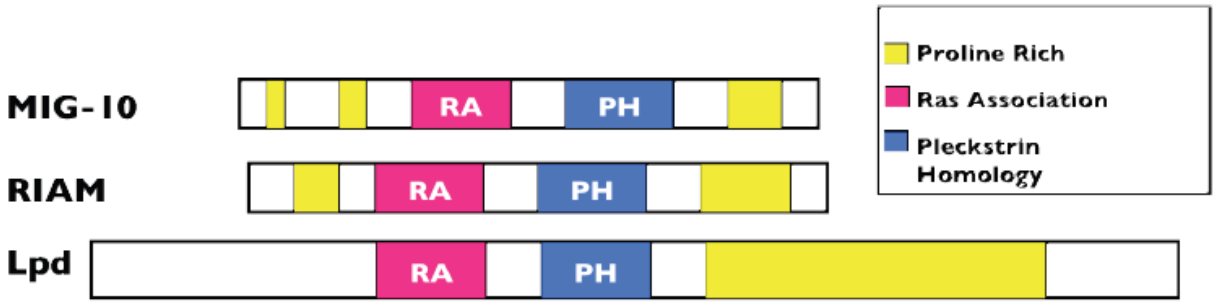

Figure 3: Domain structure of the MRL proteins (Ficociello and Ryder, unpublished data).

commonly associated with signal transduction pathways (Lafuente et al., 2004). These adaptor proteins are found downstream of cell surface molecules, indicating that they are involved in receptor activation and cellular response in axon guidance and migration (Krause et al., 2004).

Originally discovered in a screen for defective neuronal migration, the phenotype of mutations within the *mig-10* gene indicates its role in not only neuronal migration, but also excretory canal growth and axon guidance (Manser et al., 1997; Manser & Wood, 1990). Mutations within the *mig-10* gene result in incomplete migration of three neurons that undergo long range anteroposterior migration during embryogenesis: CAN, ALM, and HSN. Both the CAN and ALM migrations occur anterior to posterior whereas HSN occurs posterior to anterior (Manser & Wood, 1990). This suggests that MIG-10 affects the migration mechanism. Mosaic analysis in this paper suggested non-autonomous function in the excretory canal, which suggests that MIG-10 functions within epidermal cells, possibly as a role in signal transduction of target cells or the migratory path (Manser et al., 1997).

Mutations in the *mig-10* gene also result in defects in the EC outgrowth, with truncation in both anterior and posterior outgrowth. This truncated outgrowth is similar to mutations affecting axon guidance, such as mutations within the *unc* genes (Hedgecock 1987). Defects in axon guidance are also found in *mig-10* mutants, such as irregular branching in the HSN and loss of axonal branching in the AVM (Chang et al. 2006). The phenotype presented by defects in the *mig-10* gene is similar to phenotypes presented within other animals with known defects in genes responsible for axon guidance.

Defects in migratory neurons are the result of recessive alleles of *mig-10*. Presently, there are four recessive alleles of the gene, all of which are characterized by the truncation of cell migration, though the severity varies with alleles. *Mig-10(ct41)* shows the strongest defects in excretory canal truncation as a result of an amber stop codon, effectively destroying protein function (Manser et al. 1997). The *e2527* allele was discovered in a screen with the canonical *ct41*allele, and shows a significantly less severe defect in excretory canal truncation (Manser et al. 1997). The *mig-10(mp0920)* was isolated through EMS mutagenesis in order to produce point mutations in *C. elegans*. Excretory canal truncation and migration effects are less severe than the *ct41* mutation, likely indicating that it is a missense mutation as opposed to a null mutation (Kukla, 2009).

MIG-10 Isoforms

Three isoforms of MIG-10 have been identified: MIG-10A and MIG-10B, and MIG-10C (Figure 4). The transcripts of these isoforms are expressed through different promoter regions

and have differences in their initial exons (Quinn et al., 2006). The protein isoforms differ in their N-terminal regions, with additional proline rich regions in MIG-10A and MIG-10C. MIG-10C has not been shown to be necessary for MIG-10 function to this point. Fosmids, genetic constructs consisting of the genomic sequence surrounding a gene, containing MIG-10A and MIG-10B isoforms together have been shown to have the ability to rescue *mig-10* mutant phenotypes (Zhang 2010). These conclusions show the importance of the different isoforms in the development of a functional nervous system in *C. elegans*. These conclusions have also led to the question of the ability of MIG-10 isoforms to rescue excretory canal truncation, a phenotype of *mig-10* mutants, cell autonomously.

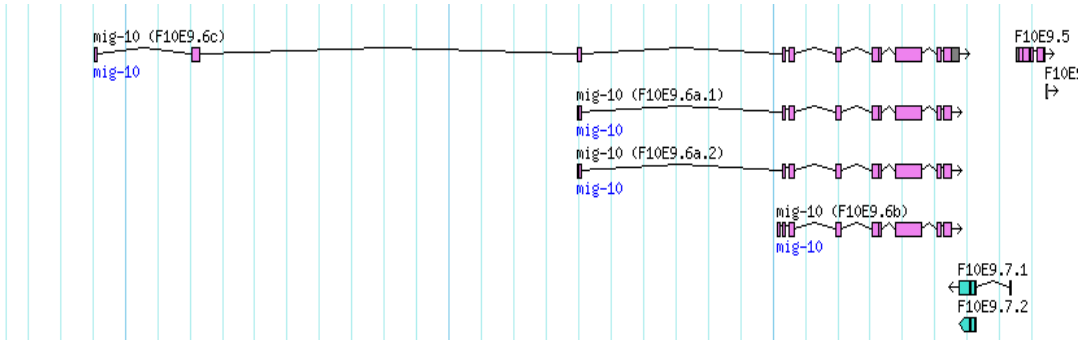

Figure 4. *mig-10* transcripts
The three *mig-10* transcripts (A,B, and C) are shown at the top of the figure. Purple boxes represent exons. Transcript *mig-10a.2* is identical to *mig-10a.1*, except that the non-coding region is 2 bps longer. Taken from Wormbase (http://www.wormbase.org/)

MIG-10: Pathway and Function

The domain binding regions in MIG-10 include a Ras-interacting domain, lipid binding plexstrin homology domain, and a proline rich region, similarly to vertebrate homologs RIAM and Lpd as shown in Figure 3 (Krause et al., 2004; Quinn, 2008). The Ras-interacting domain interacts with GTPase CED-10 (Quinn, 2008). The plexstrin homology domain binds to the membrane phospholipid PI(3,4)P, which is likely phosphorylated by AGE-1, the *C. elegans* homologue of PI3 kinase (Krause et al., 2004). The MRL family is likely to play a role in actin polymerization. The protein family is known to interact with Ena/VASP protein family, most likely through the binding of the proline rich region to the EVH1 region of the Ena/VASP proteins (Krause et al., 2004; Quinn et al., 2006).

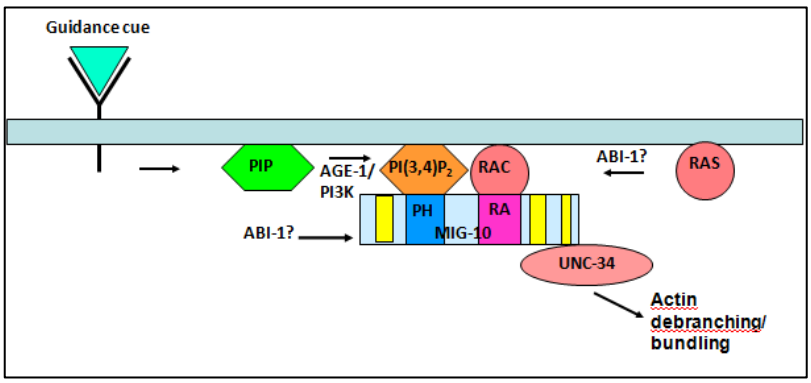

Figure 5. Proposed model for MIG-10 function. CED-10/Rac GTPase and PI3 kinase are activated in response to a guidance cue, resulting in localization of MIG-10 and related proteins to the cell membrane (McShea and Ryder, unpublished data).

During axon outgrowth, MIG-10 functions downstream of guidance cues UNC-6/netrin and SLT-1/Slit and their respective receptors UNC-40/DCC and Robo (Chang et al. 2006; Quinn et al. 2006; Quinn et al. 2008). In the absence of these guidance cues, overexpression of MIG-10 results in the formation of undirected processes, indicating its role in the promotion of outgrowth. This outgrowth can be polarized through the addition of either guidance cue, resulting in the formation of a single process (Quinn et al. 2006). MIG-10's role in this signaling pathway indicates that the protein is involved in actin polymerization. In the double mutant *mig-10; unc-34*, axon guidance defects are far more severe, indicating that MIG-10 works in conjunction to UNC-34/Ena despite distinct functions (Chang et al., 2006). The interaction of MIG-10 with the membrane phospholipid PI3K, AGE-1, showed that overexpression of MIG-10 causes excessive axon growth. A null mutation in AGE-1 suppresses excessive growth, which indicates that MIG-10 works downstream of the protein.

A proposed model for the MIG-10 signaling pathway (Figure 5) indicates that an extracellular guidance cue activates the UNC-40/DCC receptor. This in turn asymmetrically activates PI3K and CED-10/Rac GTPase. PI3K is most likely AGE-1, due to evidence that indicates a null mutation in AGE-1 suppresses excessive outgrowth of axons from an overexpression of MIG-10 (Chang et al., 2006). The asymmetric activation of Rac triggers the asymmetric localization of MIG-10. MIG-10 then associates with the Ras-related protein and PI(3,4)P2 phospholipids produced by the PI3 kinase through its Ras-interacting domain and pleckstrin homology domain. UNC-34 and ABI-1 localize through binding to MIG-10, resulting in localized actin polymerization (Quinn et al., 2006).

Actin Polymerization

Actin polymerization, the binding of actin monomers into polymers, is a complex process that stems from the presence of growth factors around the lamellipodium. As seen in Figure 6, RTKs present on the surface act as a binding location for such factors, and thus start a cascade of events which result in Rac localization and actin polymerization. As the growth factor binds

the external domain of RTK, its cytoplasmic domain becomes activated and, in turn, binds SH2-domain-containing adaptor proteins present in the cytoplasm. One of such proteins is PI3-K, and, when is becomes activated by the binding, it then converts PIP2 into PIP3. The formation of PIP3 creates a gradient localized at the migrating edge of the lamellipodia which, in turn, binds to a complex of proteins, containing the GEF Sos-1 as well as other proteins such as Abi-1 and Eps8, which then work to activate Rac (Disanza et al., 2005). Through previous experiments, the MIG-10 protein has shown to interact with ABI-1. (Gosselin & O'Toole, 2008) MIG-10 has also been associated with UNC-34/enabled/VASP, which are all downstream of Rac (Quinn 2006). These direct interactions and association, coupled with the inability of *mig-10* mutant nervous systems to develop correctly, suggests that MIG-10 also plays an important role in actin polymerization.

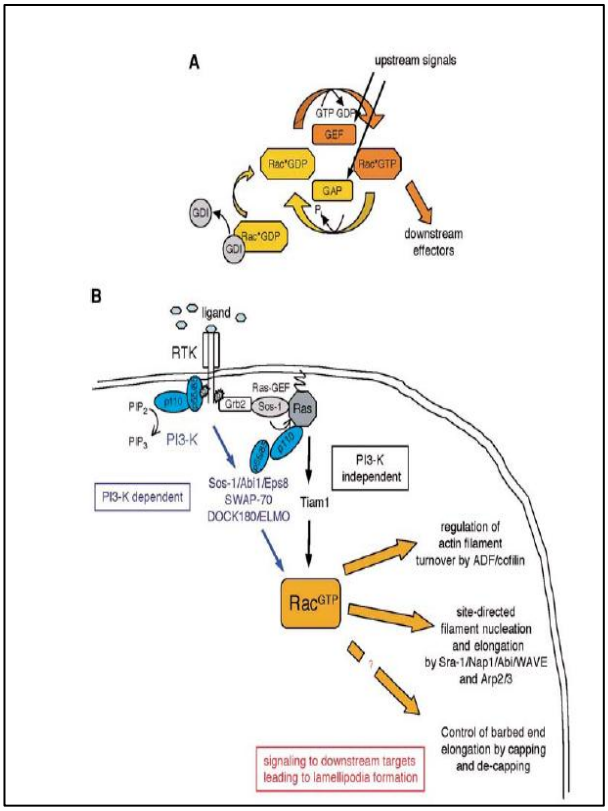

Figure 6: Schematic for Rac Activation (Disanza, A. et. al, 2005).

The cytoplasmic domain on RTK has also been shown to bind the SH2-domain of Grb2. Once bound, Grb2 binds to Sos-1 which then binds the Ras GTPase. Ras then binds to Tiam1 GEF which, in turn activates Rac (Disanza et al., 2005). The RTK and Ras-mediated pathways both end with the activation of Rac. With the activation of Rac comes three separate pathways which work together to localize and polymerize actin. Rac regulates ADF/cofilin which depolymerizes the rear end of actin filaments. Rac regulates Arp2/3 which attaches to the sides of actin filaments and allows for branching of the filament into multiple directions. Lastly, Rac regulates the capping of actin side branches which results in the termination of that particular branch. These three processes, regulated by Rac, and its interactors, work to breakdown ADP-Actin from the rear end of the actin filament so it can later be converted into ATP-actin and added to the migrating front of the actin filament and branch and cap the actin filament to allow for directional movement (Disanza et al., 2005).

UNC-53 as an Interactor of MIG-10

UNC-53 is a 1654 amino acid long protein containing 23 exons (Figure 7). These exons create a calponin homology domain, two actin binding sites, two SH3b sites, which have been known to bind signaling proteins, two CC regions and an AAA site. Together, these create a protein that is known to affect signaling pathways during neuronal development in *C. elegans* (Stringham, 2008). UNC-53 has been shown to interact with ABI-1, as well as function within the same cells of the organism (Stringham, 2008). ABI-1, through a yeast two hybrid screen, has also shown to directly interact with MIG-10 (Gosselin and O'Toole, 2008).Mutations in *unc-53* have been shown to disrupt the commissures of mechanosensory neurons and therefore create a rather disorganized and dysfunctional nervous system. In addition, *unc-53* and *mig-10* have similar phenotypes of a truncated EC (Schmidt 2008).

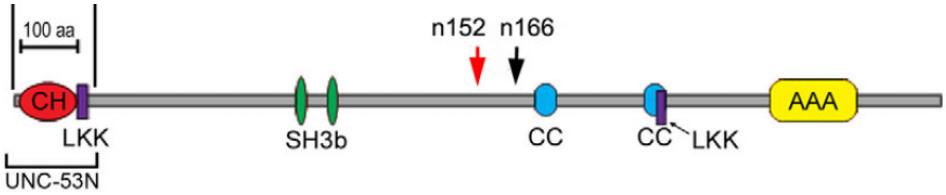

Figure 7: Domain structure of *unc-53* (Schmidt 2008)

In addition to directly interacting with ABI-1, UNC-53 has also been shown to interact with GRB2 (Stringham, 2008). Both ABI-1 and GRB2 are known to work upstream of Rac, one of the main interactors in actin polymerization, through its interaction with ARP2/3. (Disanza, A. et al., 2005) UNC-53 is thought to act in a scaffolding manner, coordinating upstream signals and using them to organize proteins, such as ABI-1, and subsequently the polymerization of actin in the cytoskeleton (Stringham, 2008). Interacting with ABI-1, UNC-53 works to control anterior-posterior migration of the ALM and PLM mechanosensory process outgrowth as well as the EC in *C. elegans* during their developmental stages (Stringham, 2002). UNC-53's role as a scaffolding protein, along with its interaction with ABI-1 and role in process outgrowth shows its importance in actin polymerization in *C. elegans. unc-53*, having a similar phenotype to and interacting with similar proteins as *mig-10*, has led us to investigate the way in which UNC-53 and MIG-10 may interact.

Project Goals

Project Goal A: Examine the role of MIG-10 in the Outgrowth of the Excretory Canal

The excretory cell is born at about 270 minutes after cleavage at which point the excretory canal proceeds to extend outwards anteriorly and posteriorly (Sulston, 1983). *mig-10(ct41)* was used to determine when MIG-10 function is required during the development of the excretory canal. The outgrowth was compared in wild type and *mig*-10 mutants using the morphological stages of embryogenesis established by Sulston.

Project Goal B: Determine if UNC-53 and MIG-10 work in overlapping pathways.

mig-10 and *unc-53* have been shown to have similar phenotypes and interact with proteins required for actin polymerization in *C. elegans*. In this project goal, we investigated whether MIG-10 and UNC-53 work in overlapping pathways to guide mechanosensory cell migration and excretory cell outgrowth. We performed a series of experiments examining both single and double mutants and analyzed the differences in migrations of their AVM, ALM, PVM, and PLM mechanosensory neurons as well as the differences in the outgrowth of the EC.

Project Goal C: Determine the ability of *mig-10* isoforms to cell autonomously rescue *mig-10* defects

Previous studies have shown the ability of MIG-10A and MIG-10B isoforms, when introduced together, to rescue truncation of the EC in *mig-10* mutant animals. (Zhang, 2010). These previous experiments utilized fosmids to deliver the isoforms into the mutant strains. The use of such techniques allows for the expression of MIG-10AB in all cells which naturally express the *mig-10* gene. Through the use of *mig-10A* and *mig-10B* cDNA, this project goal aimed to test the ability of MIG-10AB to cell autonomously rescue EC truncation in *mig-10* mutants.

Methods

Maintaining Strains

Strains of *C. elegans* used in this project were maintained on Nematode Growth Medium (NGM) agar plates spotted with *E. coli*. Active strains were maintained twice a week by transferring three L4 hermaphrodites to new plates and stored at 20°C. Inactive strains were maintained once a week and were kept at 15°C. Strains which had starved were chunked and allowed to go through a few generations before being used in studies.

Preparation of Embryos for Quantification

Embryos were prepared for quantification by growing up plates of gravid hermaphrodites. Worms were then washed off the plates and into 15 ml conical tubes with M9 solution. The conical tubes were then centrifuged for 2 minutes at 500xg (1,500 rpm) and the supernatant drained. The wash was repeated twice and 10 ml of .1 M NaOH/10% bleach was then added to the conical tubes. Conical tubes were vortexed every 30 seconds for 6-7 seconds until gravid worms were digested and eggs remained. The tubes were then centrifuged for 2 minutes at 1,500 rpm and the bleach supernatant was immediately removed. 10 ml of M9 solution was added to each conical tube and the tubes were once again centrifuged for 2 minutes at 1,500 rpm. The supernatant was removed and M9 solution was added, repeating the process two more times. After the third wash, excess supernatant was removed and the eggs were resuspended at a convenient volume. Eggs could then be pipetted to slides for analysis or to plates for timed growth.

Preparation of L1 Larva for Timed Growth

After the completion of the egg prep, eggs were then placed onto a ceramic strainer, which was located in a glass petri dish filled with M9 solution. Once the eggs hatched, worms fell through the strainer and into the M9 solution. These were then added to a 15 ml conical tube and centrifuged to later place the worms onto NGM plates for timed growth.

Preparation of Worm Slides for Quantification

Quantification of worms was performed using L4 hermaphrodites that were placed on agarose slides. To make the slides, 20 µl of 1M sodium azide was added to 2 ml of heated 2% agarose and vortexed. A drop of agarose with azide was added to a slide and covered with another to seal the pad. Worms were either picked or pipetted onto slides. To pick worms, 3-5 ul of M9 solution was placed onto the agarose and worms were picked directly from the plate and

onto the slides. To pipette worms, worms were washed into a 1.5 ml centrifuge tube with M9 and allowed to settle. 3-5 ul of worms were then pipetted onto the agarose pad. A cover slip was placed over the over them to ensure the worms remained in a lateral position. In the second method, worms were washed off the plate and into a 1.5 ml microfuge tube with M9. Once the worms settled to the bottom of the tube, 3 µl of worms were pipetted onto the pad. A cover slip was then placed over the slide to ensure the worms remain in a lateral position.

Rescue Cross

To determine the ability of MIG-10A and MIG-10B to cell autonomously rescue excretory canal truncation, a mixture of cDNAs was injected directly into the ovaries of adult hermaphrodites. The progeny which retained the array were then genetically crossed into a *mig-10* mutant background. The strategy for this genetic cross can be seen in Figure 8, for one injection resulting in the array named mpEx1001.

GOAL: mpEx1001; *mig-10; pgp-12::GFP*

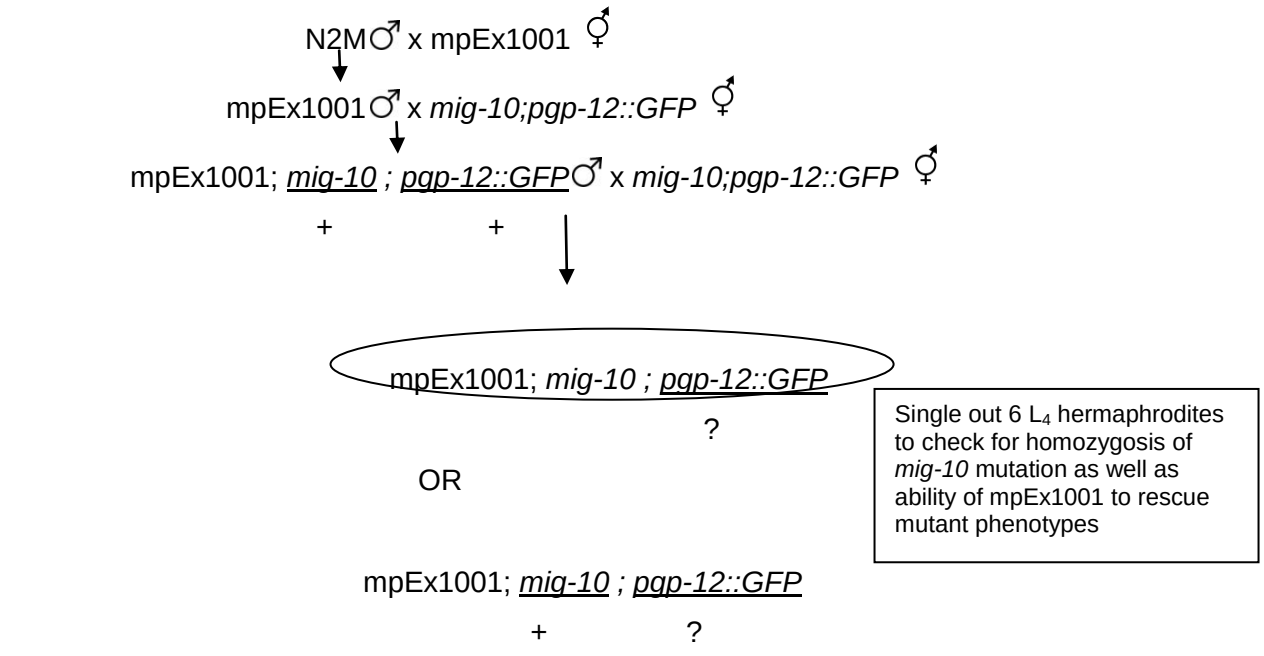

Figure 8: Cross to generate mpEX1001;*mig-10;pgp-12::GFP*

Quantification of Phenotypes

Prepared slides were examined under a compound microscope using the standard bright field as well as epifluorescence. Bright field was used to identify the age of the worm, as well as to determine the total length, distance between the center of the vulva to the back of the pharynx, and the distance between pharynx to the tip of nose. Epifluorescence was used to quantify the phenotype of interest through measurement of cells labeled by fluorescent transgenes, such as length of the excretory canal (*pgp-12::GFP*) or the position of migrations of ALM1, ALM2, AVM, PVM, and PLM cells (*flp-20::GFP*). The outgrowth of the PLM process was also examined. Quantifications were done using the ImageJ software, which measured the distances in pixels.

In the analysis of excretory cell truncation, the length of excretory cell was measured both anterior and posterior from the cell body. The distance between worm pharynx to the tip of its nose and the total length of the worm were also measured to normalize the truncation data, respectively. In the analysis of mechanosensory cell migrations, distance from vulva to the final location of ALM1, ALM2, AVM, PVM, and PLM cell bodies were measured and normalized with the distance from the posterior of the pharynx to the middle of the vulva. The PLM process outgrowth was examined on the basis of whether or not it surpassed the distance to the vulva. If the process passed the vulva, it received a value of +1. Terminating within the vulval region would result in a value of 0 and posterior of the vulva would result in -1.

Statistical Analysis

Statistical analysis was run on the normalized data from the worm ImageJ measurements. Tests such as the One-way ANOVA, and the Tukey Post Hoc tests in the program SPSS were used. The null hypothesis was that there was no difference in the length of the excretory cells and the neuronal cell migrations in the different strains. The strains whose post-hoc tests had a p-value of less than 0.05 ($p<0.05$) were viewed as being significantly different from one another, while those whose p-value was greater than 0.05 ($p>0.05$) were not significantly different.

Results

mig-10(ct41) truncates the excretory canal during embryogenesis

Previous studies have indicated that mutations in *mig-10* truncate the excretory canal. Under the hypothesis that this truncation would be prominent at early stages of development, gravid hermaphrodites were lysed in order to isolate eggs for timed growth. Wild type embryos, containing the transgene pgp-12::GFP, were used as a control to compare relative outgrowth during stages of embryogenesis. *mig-10; pgp-12::GFP*, which contains the null allele *ct41*, was used to observe excretory canal truncation. Starting from the 1.5 fold stage, the first morphological stage at which the excretory cell was visible by GFP labeling, outgrowth was evaluated until late L1 larva (Figure 9). Measurements were taken of both the anterior and posterior process and were not normalized in order to allow a direct comparison of absolute process length at all stages.

In the wild type embryo, the anterior process was not visible until the 2 fold stage, and growth continued well into the late L1 stage (Figure 9A). *mig-10* mutants showed visibility of the anterior process during the 2 fold stage as well, indicating almost no visible difference between the two strains at this stage. At this point in development, the outgrowth was too minimal to suggest that the null mutation plays a critical role. Truncations due to mutations in *mig-10* were apparent by the 3 fold stage, and while outgrowth continued during later stages, this truncation remained prominent. . It also appeared that the rate of extension between stages was less than that of wild type worms.

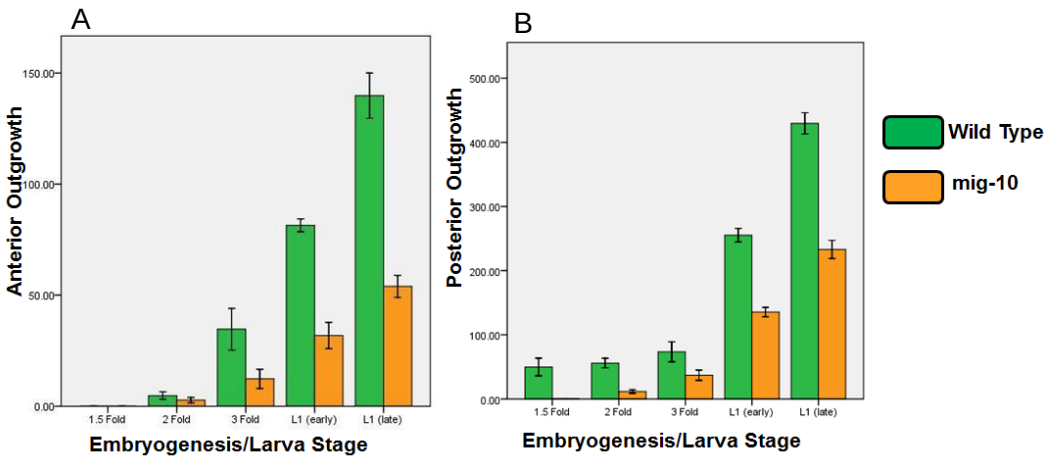

Figure 9: Excretory canal process outgrowth is delayed and truncated during embryogenesis. Wildtype and *mig-10 (ct41)* mutant embryos with the transgene PGP-12::GFP were observed at three different morphological stages and the L1 stage in order to quantitate excretory canal outgrowth. A) Anterior outgrowth of the excretory canal. Measurements were taken from the anterior end of the excretory canal to the anterior end of the process. B) Posterior outgrowth of the excretory canal. Measurements were taken from the posterior end of the excretory canal to the posterior end of the canal process. Wildtype data is in green, *mig-10* data is in orange. Data were not normalized to allow for direct comparisons of length at all stages. Error bars are ± 1 standard error. n = 40 for all worms.

The posterior process in wild type *C. elegans* was first visible at the 1.5 fold stage, and showed a minimal increase in outgrowth until the L1 stage (Figure 9B). During the larval stage, the canal almost doubled its length. In *mig-10* mutants, the posterior process was not visible until the 2 fold stage, and truncation was already apparent at this stage. In contrast, the anterior outgrowth at the same stage showed no apparent differences in length between wild type and *mig-10* mutants. This suggested that *mig-10* is essential to normal posterior outgrowth at this stage of embryogenesis. Later stages of development also indicated truncation in the *mig-10* mutants through the late L1 stage. Truncation seen in both anterior and posterior outgrowth suggested that the effects of *mig-10* mutations were first noticeable during the 1.5 fold stage, early on in development. The continued truncation throughout development further suggested that mig-10 function is essential to normal outgrowth for both processes.

mig-10 (ct41) reduces the rate of excretory canal outgrowth in *C. elegans* during embryogenesis

We next sought to explore whether the rate of outgrowth during development was also altered. Embryos isolated from lysed hermaphrodites were placed on a slide and underwent timed growth, during which repeated measurements were taken every 20 minutes on individual embryos to observe the overall outgrowth of the excretory canal (Figure 10). Outgrowth rate in wild type embryos showed a steady increase in rate during the early half of embryogenesis and began to increase exponentially during the latter half. In *mig-10(ct41)* worms, however, the rate of outgrowth remained almost constant. These results indicate that loss of *mig-10* function

results in truncation of the excretory canal through reduction of the overall rate of excretory canal outgrowth.

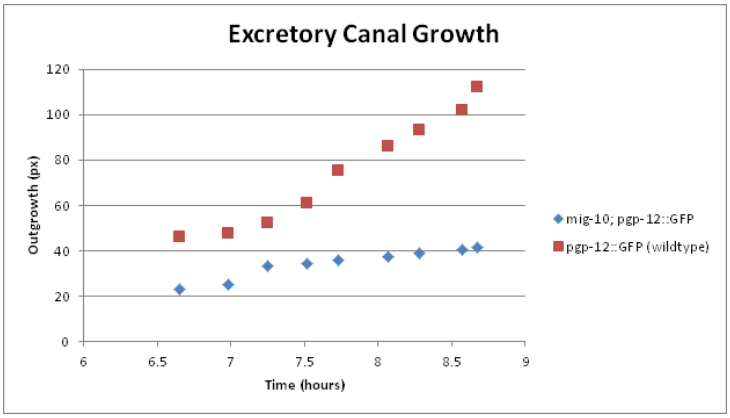

Figure 10: *mig-10(ct41)* reduces the rate of excretory canal outgrowth during embryogenesis. Wildtype and *mig-10(ct41)* mutants were measured during embryogenesis in order to compare outgrowth over time. The entire excretory canal was measured to determine the overall outgrowth. N=10 for both strains. Average values are shown at each time point.

MIG-10 and UNC-53 interact differently in anterior and posterior excretory canal outgrowth

We hypothesized that MIG-10 and UNC-53 interact in overlapping pathways, and therefore *unc-53* mutations would enhance the Mig-10 mutant phenotype of truncated process growth in the EC. To test our hypothesis, *mig-10, unc-53,* and double mutant strains were tagged with pgp-12:GFP, to mark the EC, and examined under epiflourescence. Measurements of the anterior and posterior process outgrowths were taken and, to control for worm size, normalized using the distance from the nose to the posterior of the pharynx and the tip of the nose to the tail respectively (Figure 11).

Our results suggest that UNC-53 and MIG-10 interact in a different way in the anterior process than they do in the posterior process of the EC (Figure 11). Wild type *C. elegans* have an EC that extends an anterior projection to the nose, and a posterior projection to the tail (Figure 11C). Both *mig-10* and *unc-53* mutations truncate the growth of these processes (Figure 11A,B). *mig-10;unc-53* double mutants have an enhanced truncation of the anterior projection of the EC (Figure 11A) which suggests that they work in separate pathways to guide anterior process outgrowth. Surprisingly, double mutants have a posterior process truncation that is statistically less severe than that of *mig-10* mutants (Figure 11B,F). These data show that MIG-10 and UNC-53 interact in different ways to direct anterior and posterior growth of the EC.

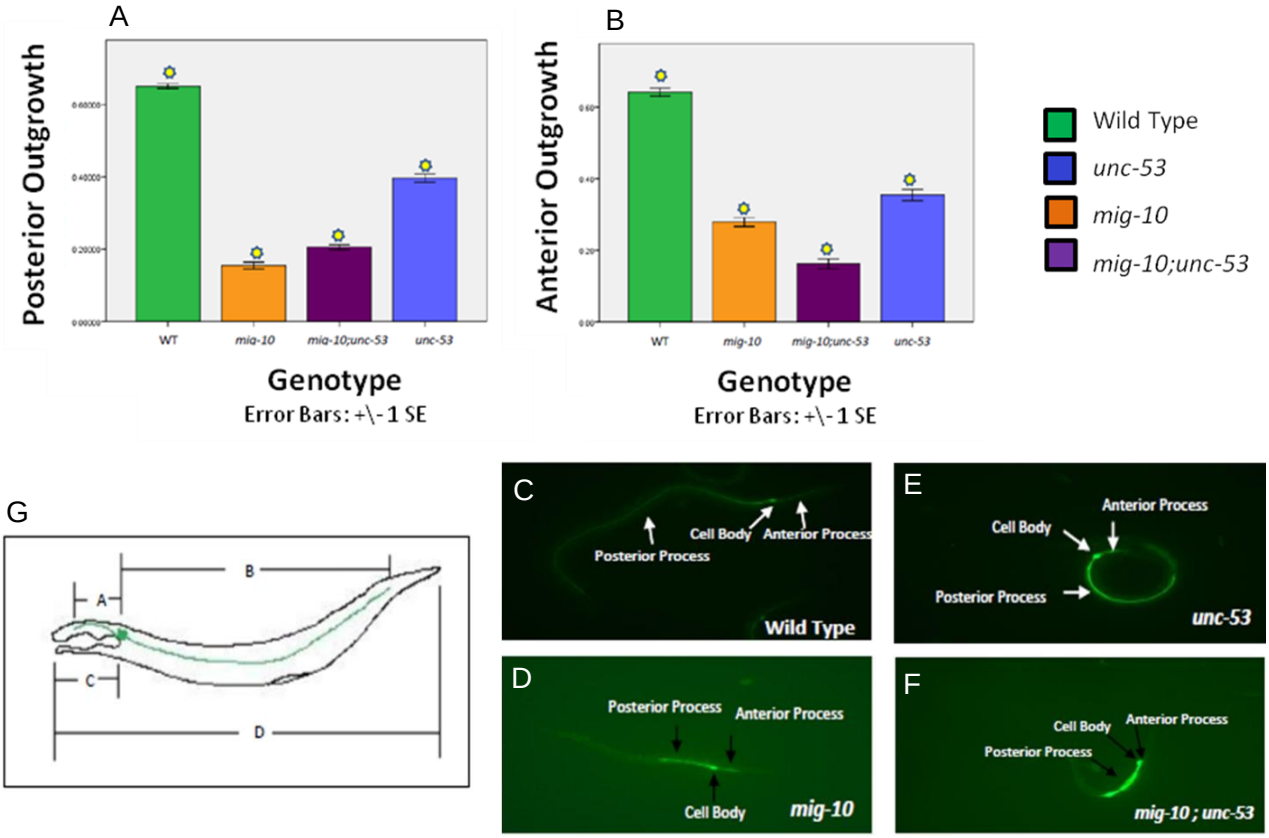

Figure 11: *mig-10;unc-53* double mutants have varied effects on EC truncation
(A) Posterior EC in mig-10;unc-53 double mutants is less truncated than in mig-10 mutants. (B) *mig-10;unc-53* double mutants enhance anterior EC truncation. (C-F) Epifluorescent photomicrographs of representative *C. elegans*. All strains have *pgp-12::GFP* transgene to mark EC (C) Wild Type (n=40) (D) *mig-10* (n=36) (E) *unc-53* (n=46) (F) *mig-10;unc-53* (n=38) (G) *C. elegans* schematic showing distance (a) EC cell body to the distal end of the anterior projection (b) EC cell body to the distal end of the posterior projection (c) tip of the nose to the back of the pharynx and (d) tip of the nose to the tip of the tail
Suns represent bars which are significantly different from all other genotypes (ANOVA, Tukey HSD Post-Hoc tests at $p<0.05$).

Interaction of MIG-10 and UNC-53 Show Varying Effects on Mechanosensory Cell Body Migration

We hypothesized that mutations in *unc-53* would enhance the Mig-10 mutant phenotype of truncated mechanosensory neuron cell body migration in *C. elegans*. To test this hypothesis, we examined and compared *mig-10, unc-53,* and double mutant strains, containing the *flp-20::GFP* transgene to label mechanosensory neurons, under epiflourescence at the L4 stage to determine the position of the AVM, ALM1, ALM2, PVM, and PLM cell bodies in relation to the vulva. These data were normalized, to control for overall body size, by the distance from the vulva to the posterior of the pharynx (Figure 12J).

Overall, Figure 6 and Table 1 surprisingly show that *unc-53* mutations (Figures 12H,I) have varying effects on (Figure 12F) mechanosensory neuron cell body migrations. In the wild type, ALM1 and ALM2 migrate posterior, while AVM migrates anterior. The PVM is involved in

two migrations, with the PVM progenitor cell first migrating posterior, and then the PVM itself migrating anterior. The PLM remains in the tail of the worm and is not known to migrate (Hedgecock et al. and Table 1). *mig-10* mutations result in the truncation of AVM, ALM1, and ALM2 migrations (Figures 12A-C). *unc-53* mutations have no significant effect on the migration of the AVM cell body. Double mutants have a truncated AVM migration similar to that of *mig-10* mutants (Figure 12A), further confirming that *unc-53* has no role in AVM migration. Interestingly, however, both ALM1 and ALM2 migrate further in *unc-53* mutants than in wild type. Additionally, *unc-53* mutations suppress the Mig-10 phenotype, having ALM1 and ALM2 migrations that are less truncated in double mutants than in *mig-10* mutants (Figures 12B,C). *mig-10* and *unc-53* mutations alone have no effect on PVM migration. Surprisingly, double mutants have a PVM that is mispositioned in relation to the wild type (Figure 12D). As expected, neither single nor double mutants affect PLM migration (Figure 12E). Taken together, these data suggest that in ALM neurons, MIG-10 and UNC-53 act in opposition to each other, while in the PVM neuron, they act synergistically.

Table 1: *unc-53* mutations have varying effects on mechanosensory neuron cell body migration (Hedgecock et al., 1987).

	AVM	**ALM**	**PVM**	**PLM**
Region of Worm	Anterior	Anterior	Posterior	Posterior
Direction of Migration	Anterior Migration	Posterior Migration	1st migration =posterior 2nd migration =anterior	None
Effects of *mig-10*	Truncation	Truncation	None	None
Effects of *unc-53*	None	Further migration than wild type	None	None
Effects of Double Mutant	Similar to Mig-10	Reduced Truncation	Mispositioned	None

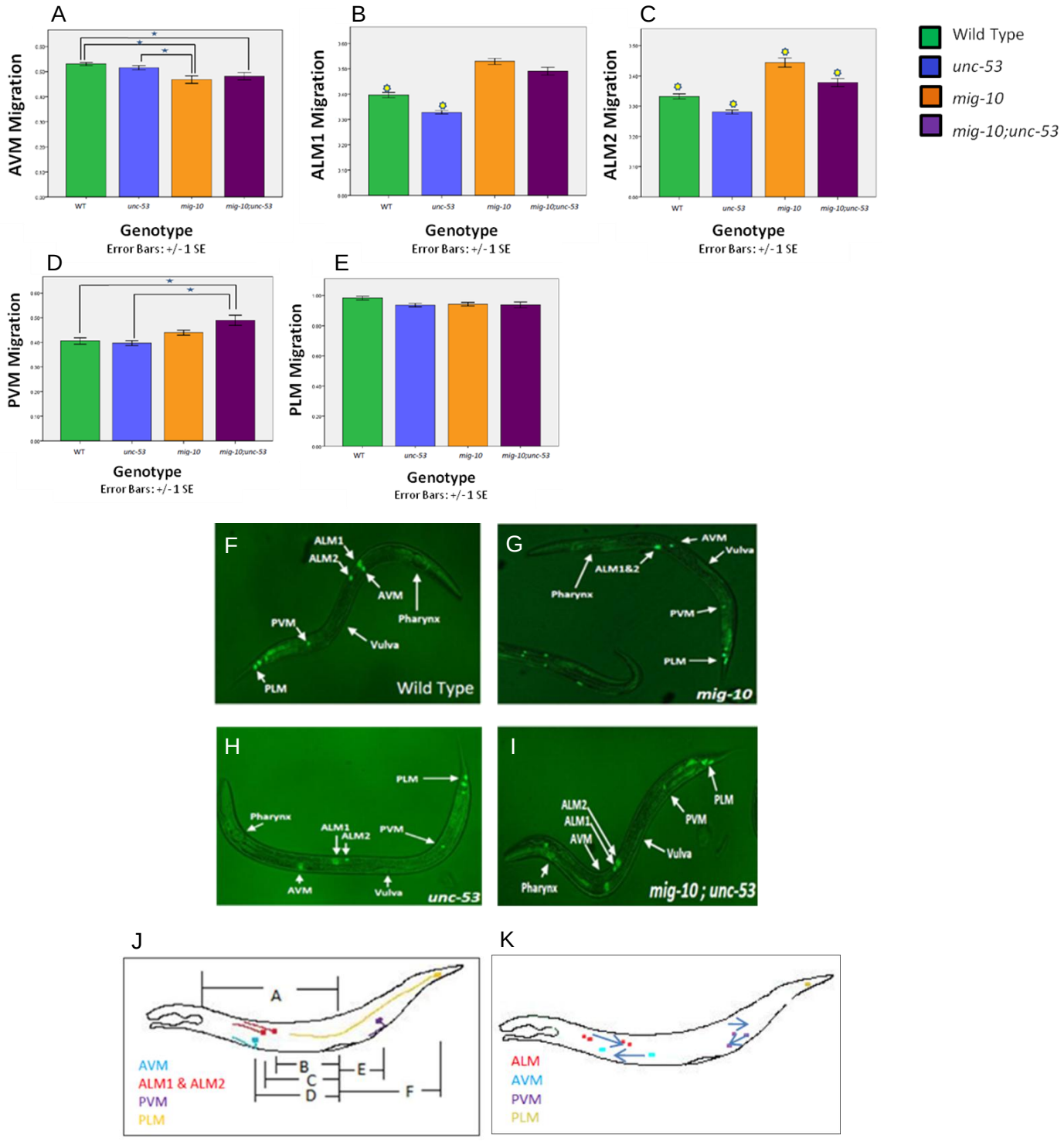

Figure 12: *unc-53* has varied effects on mechanosensory neuron cell body migration
A) *unc-53* mutations have virtually no effect on AVM cell body migration. (B) *unc-53* mutations cause the ALM_1 cell body to migrate further than that of the wild type. (C) *unc-53* & *mig-10* mutations have opposing effects on ALM_2 cell body migration. (D) *unc-53;mig-10* double mutants truncate the PVM cell body migration. (E) *mig-10* and *unc-53* mutations have no effect on PLM cell body migration. (F-I) Epifluorescent photomicrographs of representative *C. elegans*. All strains have *flp-20::GFP* transgene to mark mechanosensory neurons (F) Wild Type (n=50) (G) *mig-10* (n=50) (H) *unc-53* (n=50) (I) *mig-10;unc-53* (n=50) (J) Schematic showing positions of the Pharynx (a), ALM_2 (b), ALM_1 (c), AVM (d), PVM (e), and PLM (f) relative to the vulva (K) Schematic showing the migration of certain mechanosensory neurons. Asterisks and brackets represent mean cell body migration differences that are significant at $p<0.05$. Suns represent bars which are significantly different from all other

mig-10 and *unc-53* mutations truncate PLM process outgrowth

We also examined the effect of *mig-10* and *unc-53* mutations on PLM process outgrowth. We examined and compared *mig-10, unc-53,* and double mutant strains, containing the *flp-20::GFP* transgene to label mechanosensory neurons, under epiflourescence at the L4 stage to determine the relative lengths of the anterior projection of the PLM in relation to their position to the vulva. Wild type *C. elegans* have a PLM process that grows far anterior to the vulva. When *unc-53* is mutated, the PLM process is drastically truncated and terminates posterior to the vulva. *mig-10* mutants have a similar, though far less severe, phenotype. Double mutants have a phenotype similar to that of *unc-53* mutants (Figure 13). These data suggest that, in PLM, MIG-10 and UNC-53 are part of the same pathway.

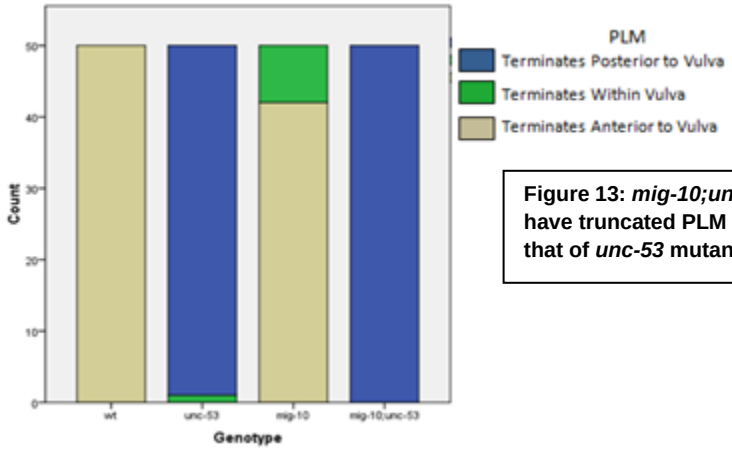

Figure 13: *mig-10;unc-53* mutant *C.elegans* have truncated PLM outgrowth similar to that of *unc-53* mutants

mig-10A and *mig-10B* together cell autonomously rescue excretory canal truncation in *mig-10* mutant *C. elegans*

Previous studies have shown the ability of *mig-10* fosmids to rescue EC truncations in *mig-10* mutant worms (Zhang 2010). Here, we tested the hypothesis that *mig-10* isoforms have the ability to cell autonomously rescue EC truncation in *mig-10* mutant worms. We created constructs expressing either *mig-10A* or *mig-10B* from the *pgp-12* promoter, which is expressed specifically in the EC (Zhao 2005). Both constructs were injected together into *mig-10* mutant worms, along with a marker construct, to generate transgenic animals. Measurements of the anterior and posterior EC processes were made as described above in both transgenic worms (*mig-10AB*) and *mig-10* mutant siblings that had lost the transgene. In wild type animals, the EC has two projections, sending one anteriorly to the nose and the other posteriorly to the tail (Figure 14E). In *mig-10* mutants the EC is severely truncated in both the anterior and posterior processes (Figure 14F). *mig-10AB* fully rescued anterior truncation of the EC (Figure 14A). *mig-*

10AB provided a wide range of partial rescue to truncation of the posterior process of the EC (Figure 14B). In both EC processes, when the array was lost, worms had a phenotype similar to *mig-10* mutants (Figure 14).

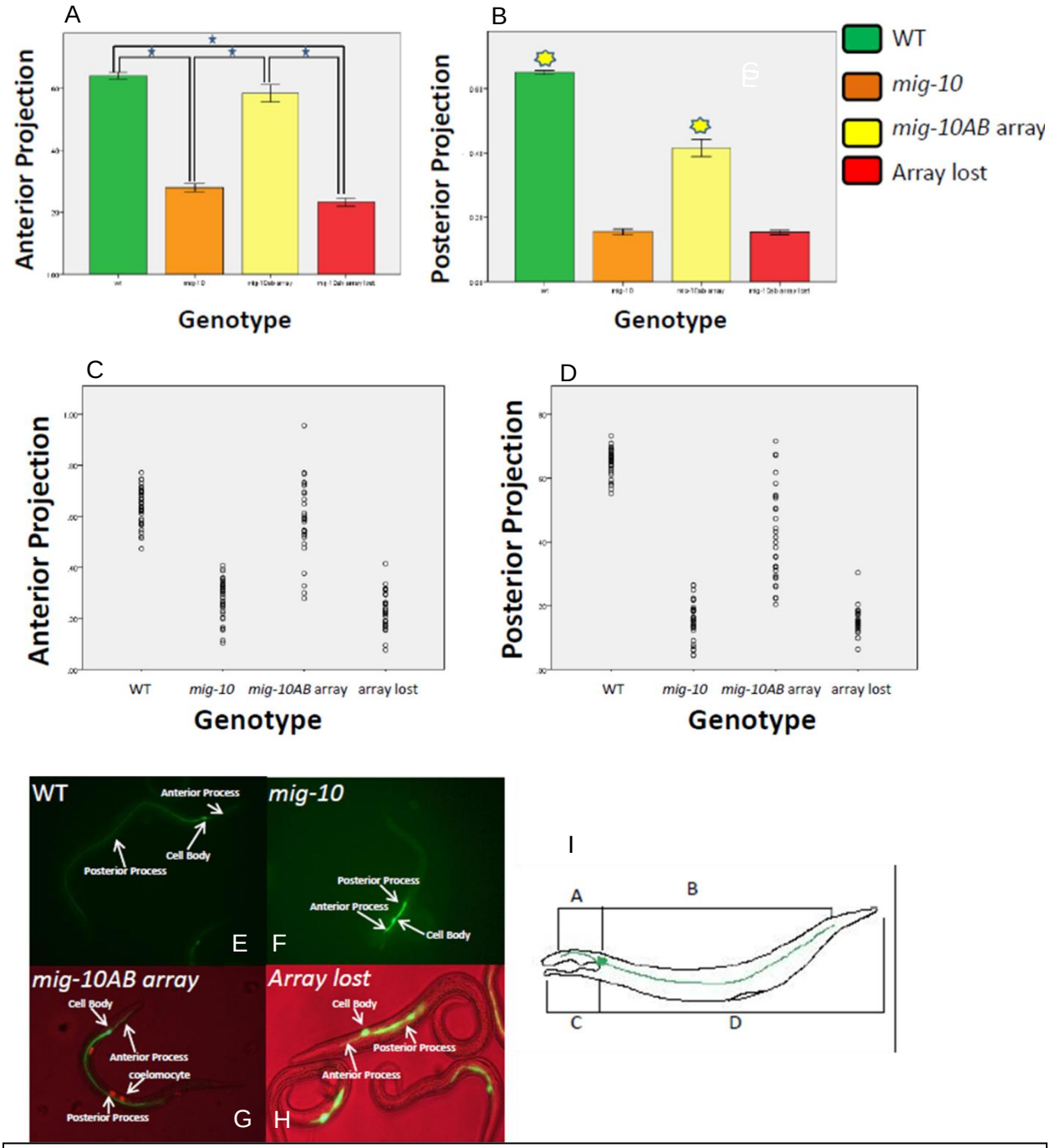

Figure 14: *mig-10AB* isoforms together have the ability to provide full cell autonomous rescue to anterior EC truncation as well as partial cell autonomous rescue to posterior EC truncation in *mig-10* mutant C. elegans
(A) *mig-10AB* isoforms together have the ability to fully rescue anterior EC truncation in *mig-10* mutant *C. elegans* (B) *mig-10AB* isoforms together have the ability to partially rescue posterior EC truncation in *mig-10* mutant *C. elegans* (C) scatterplot of the data in Panel A (D) scatterplot of the data in Panel B (E-H) Epifluorescent photomicrographs of representative *C. elegans*. All strains have *pgp-12::GFP* transgene to mark EC (E) Wild Type (n=40) (F) *mig-10* (n=36) (G) *mig-10* containing *mig-10AB* array (n=30) (H) *mig-10* after losing *mig-10AB* array (n=32) (I) *C. elegans* schematic showing distance (a) EC cell body to the distal end of the anterior projection (b) EC cell body to the distal end of the posterior projection (c) tip of the nose to the back of the pharynx and (d) tip of the nose to the tip of the tail
Asterisks and brackets signify significant differences (ANOVA, Tukey HSD Post-Hoc tests at $p<0.05$) and suns signify those bars which are significantly different to all other groups (ANOVA, Tukey HSD Post-Hoc tests at $p<0.05$)

mig-10A and *mig-10B* individually are sufficient to provide full cell autonomous rescue to anterior truncation and partial rescue to posterior truncation of the EC in *mig-10* mutant *C. elegans*

We next tested the ability of the *mig-10A* and *mig-10B* transcripts to rescue EC outgrowth individually. *mig-10A* (Figure 15A,C), as well as *mig-10B* (Figure 15E,G), are individually sufficient for full cell autonomous rescue of the anterior truncation of the EC in *mig-10* mutants. Furthermore, *mig-10A* (Figure 15B&D) and *mig-10B* (Figure 15F,H), individually, are sufficient to provide a range of partial rescue to posterior truncation of the EC in *mig-10* mutants. In all cases, once the transgene is lost, worms resemble *mig-10* mutants (Figure 15).

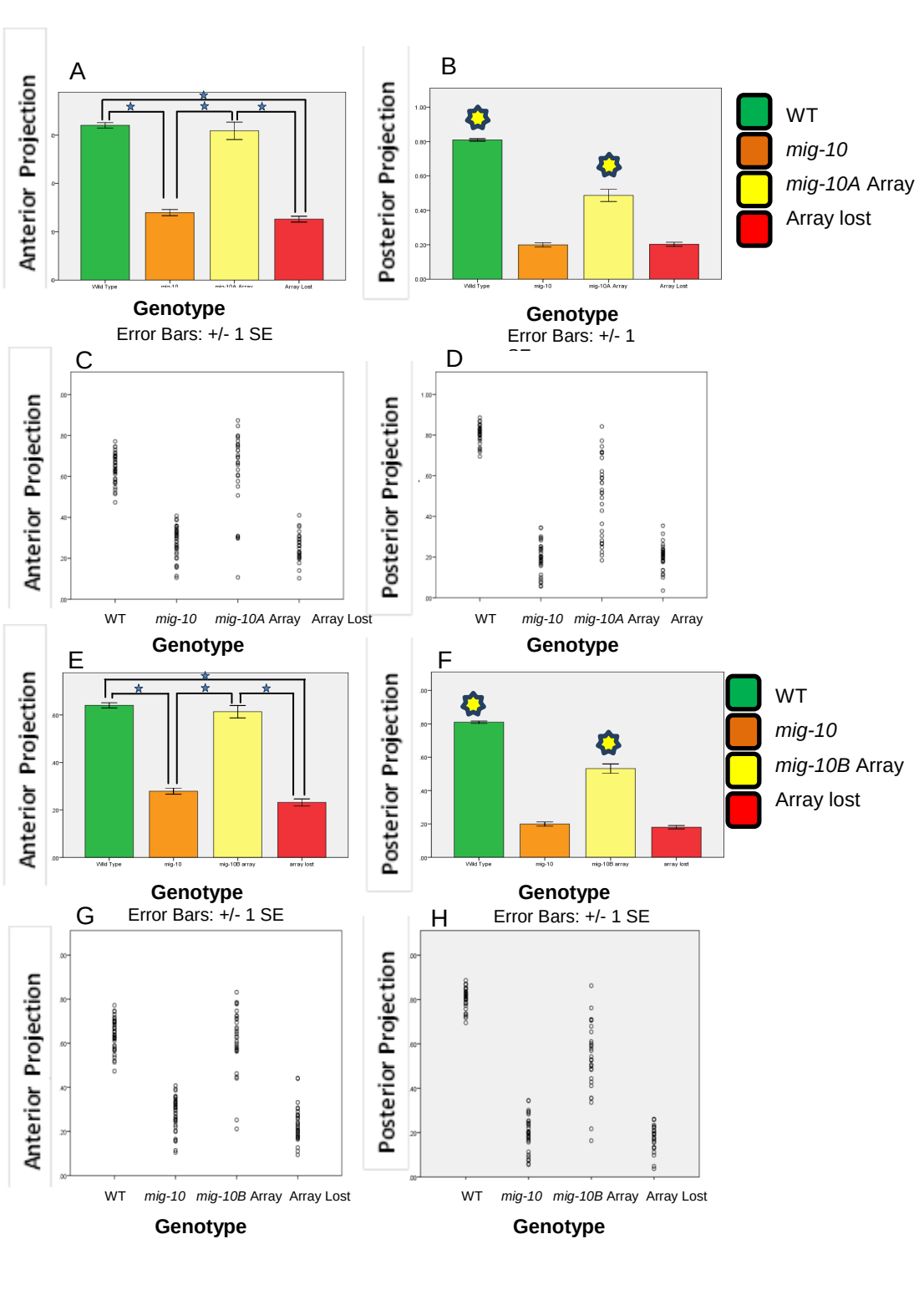

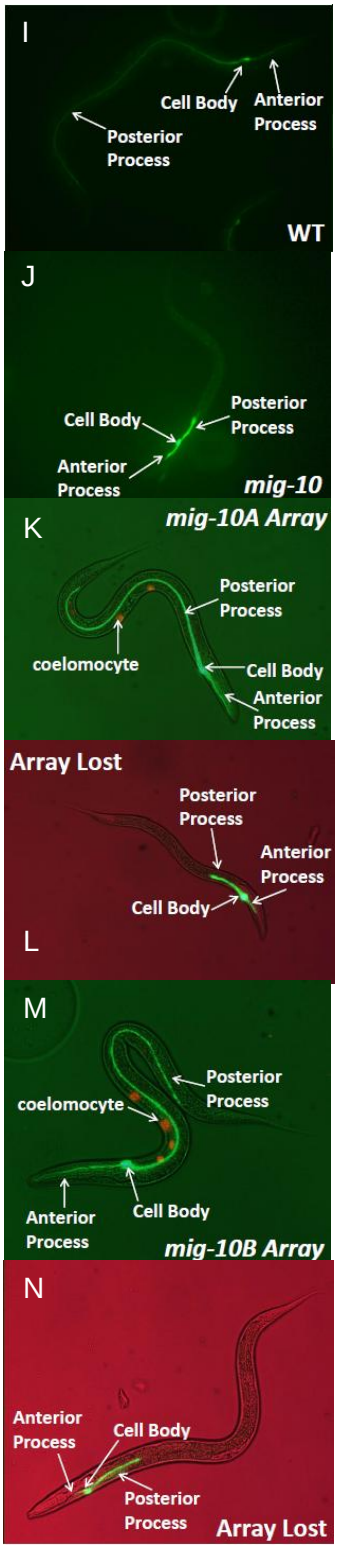

Figure 15: *mig-1A* and *mig-10B* alone are sufficient to provide cell autonomous full rescue to anterior truncation of the EC in *mig-10* mutants

(A) *mig-10A* has the ability to fully rescue anterior EC truncation in *mig-10* mutant *C. elegans* (B) *mig-10A* has the ability to partially rescue posterior EC truncation in *mig-10* mutant *C. elegans* (C) scatterplot of Panel A (D) scatterplot of Panel B (E) *mig-10B* has the ability to fully rescue anterior EC truncation in *mig-10* mutant *C. elegans* (F) *mig-10B* has the ability to partially rescue posterior EC truncation in *mig-10* mutant *C. elegans* (G) scatterplot of Panel E (H) scatterplot of Panel F (I-N) Epifluorescent photomicrographs of representative *C. elegans*. All strains have *pgp-12::GFP* transgene to mark EC (I) Wild Type (n=40) (J) *mig-10* (n=36) (K) *mig-10* containing *mig-10A* array (n=30) (L) *mig-10* after losing *mig-10A* array (n=30) (M) *mig-10* containing *mig-10B* array (n=30) (N) *mig-10* after losing *mig-10B* array (n=30) .
Asterisks and brackets signify significant differences (ANOVA, Tukey HSD Post-Hoc tests at $p<0.05$) and suns signify those bars which are significantly different to all other groups (ANOVA, Tukey HSD Post-Hoc tests at $p<0.05$)

Discussion

MIG-10 is a known component for axon guidance, neuronal migration, and excretory canal outgrowth (Manser et al., 1997). To determine if it plays a role in early development of the excretory cell, canal outgrowth of wild type embryos was compared to that of *mig-10(ct41)* mutants. Quantitative results showed that truncation was evident during embryogenesis, particularly affecting the outgrowth of the posterior process (Figure 9). These results suggest that MIG-10 is necessary for development of the excretory canal during embryogenesis and also functions differently in the anterior and posterior region of the worm.

Studies of anterior outgrowth in both wild type and *mig-10* mutants indicate that in the null mutant, outgrowth is not delayed initially, but the rate of outgrowth is slowed (Figure 9A).In the posterior process, outgrowth is delayed and also shows signs of a slower rate of growth. During embryogenesis in the wild type, the posterior canal undergoes a gradual outgrowth that does not increase until late in embryogenesis. The change in increase appears to correlate with later embryogenesis development (Figure 9B, Figure 10). This outgrowth does not increase until the L1 stage, where the process extends to almost double its length. Overall, outgrowth is delayed in the posterior, but not in the anterior, suggesting a difference in *mig-10* function in the anterior and posterior regions. Comparisons of the rate of outgrowth indicate that the mutant is slower than the wild type during embryogenesis (Figure 10). It appears that this rate may continue to remain the same during later stages of development. Therefore, proper MIG-10 function is needed almost at the start of excretory canal growth and throughout embryogenesis. Truncation is most likely due to the slow rate of outgrowth, since MIG-10 normally seems to function to increase outgrowth rate.

Since this study did not examine the completion of the excretory canal development, further studies would be necessary in order to shed light on how MIG-10 affects the completion of outgrowth, and canal elongation as the embryo continues to grow. The use of the null mutant *ct41* in comparison of excretory canal outgrowth during embryogenesis suggests that a complete lack of a functioning MIG-10 slows overall outgrowth. Additional alleles of *mig-10*, such as *e2527* and *mp0920*, could be used to indicate if a partially functioning protein is sufficient for outgrowth.

Through Project Goal B we set out to explore the interaction between MIG-10 and UNC-53. The acts of cell migration and process outgrowth have been shown to be affected by the presence of both MIG-10 and UNC-53. In these functions, another key protein shown to have an effect is ABI-1. Previous studies have shown through a yeast-two-hybrid screen that MIG-10 and ABI-1 have a physical interaction (Gosselin & O'Toole 2008). *Abi-1(RNAi)* enhances the

effect of *mig-10* mutations, suggesting that the two proteins work in overlapping pathways (Dubuke and Grant, 2009). Additionally, UNC-53 and ABI-1 have been shown both to physically interact and to act in the same pathway (Stringham 2008). With these findings, we hypothesized that MIG-10 and UNC-53 interact in overlapping pathways, and therefore *unc-53* mutations would enhance Mig-10 mutant phenotype.

We tested this hypothesis through three experiments, where we examined the anterior and posterior process outgrowth of the EC (Figure 11), the migration of certain mechanosensory neuron cell bodies (Figure12), and the anterior outgrowth of the PLM (Figure 13). Overall, these data have shown that MIG-10 and UNC-53 interact differently in different cells. In Figure 11 we showed that worms that are *mig-10;unc-53* double mutants have an enhanced anterior process truncation of the EC. This figure also shows that double mutants have a posterior migration that is statistically less ($p<0.05$) truncated than the *mig-10* single mutants. When examining mechanosensory neuron cell migration, we found that *unc-53* does not act in the cell migration of the AVM (Figure 12A). We also show (Figure 12D) that PVM is mispositioned only in double mutant strains. Furthermore, worms mutant for *unc-53* have an ALM migration that is further than that of wild type and double mutants have an ALM migration that is further than *mig-10* single mutants (Figure 12B,C). Neither single mutants nor double mutants had any change in PLM position (Figure 12E), though *unc-53* mutations are shown to truncate the anterior PLM process outgrowth (Figure13).

These data show that MIG-10 and UNC-53 interact in a different way depending on the cell being considered. A possible model is that MIG-10 and UNC-53 act in opposition to each other in posterior migrations, while acting in synergy in anterior migration. Most of our data support this model. Cells with a posterior migration, ALM1 and ALM2 (Figure 12B,C), or posterior outgrowth, posterior process of EC (Figure 11A), have a double mutant phenotype which is statistically less truncated than the *mig-10* mutant phenotype. In the case of the ALM, *unc-53* mutant cells also travel further than those of the wild type (Figure 12B,C). In contrast, there is enhanced truncation of anterior growth of the EC in double mutant animals (Figure 11B). Lastly, the PVM is mispositioned posterior in double but not in either single mutant (Figure 12D). This mispositioning could be a result of MIG-10 and UNC-53 being required to work in synergy to control the anterior portion of the PVM migration.

Further experiments need to be completed to better understand the way in which MIG-10 and UNC-53 interact. As mentioned, previous experiments have shown that MIG-10 and UNC-53 both interact with ABI-1. A possible future experiment could entail exploring the ability for MIG-10, UNC-53, and ABI-1 to form a complex. Due to UNC-53 being a large protein, a Co-

IP may have to test certain UNC-53 domains separately. That being said, this experiment has the ability to show if MIG-10 and UNC-53 interact through a mutual interaction with ABI-1 or by separate interactions with ABI-1 depending on what complexes form.

Our data also shows that cells with posterior migrations or posterior outgrowths have double mutants that are less severely truncated than *mig-10* single mutants and, in the case of the ALMs, *unc-53* mutants actually migrate further than the wild type (Figures 11&12). This, compared to effects on anterior migrations and outgrowths, shows that UNC-53 may be part of a different mechanism in posterior movement than in anterior movement. With UNC-53 being in a different pathway, its interaction with MIG-10 will also differ. Signal transduction pathways are initiated by interaction of surface receptors with various extracellular signals. A further study of the surface receptors activated during anterior vs. posterior movement will further show if there are different pathways activated between the two.

PVM cell body migration is not affected by *mig-10* or *unc-53* but is changed in double mutants (Figure 12D). This particular mechanosensory neuron cell body is unique in that it has two migrations during development (Hedgecock, 1987). The PVM progenitor cell QL first migrates posteriorly, while PVM itself migrates anteriorly. Migration may only be affected in double mutant strains due to this uniqueness in migration pattern. An alternative interpretation could be that one mutation may not be significant enough to truncate the overall migration because it only affects one of the migrations and the other migration makes up for the loss. Further studies tracking PVM's embryonic and larval migration could shed some light on when migratory truncations are noticed in both single and double mutants. These studies, along with showing if MIG-10 and UNC-53 interact differently in anterior vs. posterior migrations, will show if they are active during embryonic or larval migration.

In Project Goal C, we set out to explore the ability of *mig-10* isoforms A and B to cell autonomously rescue the *mig-10* mutant phenotype of truncated EC growth. Previous fosmid experiments have shown the ability of *mig-10:*FosAB to fully rescue EC truncation in *mig-10* mutant worms. These experiments further showed the inability for either isoform alone to rescue truncation (Zhang, 2010). We hypothesized that *mig-10* isoforms have the ability to cell autonomously rescue EC truncation in *mig-10* mutant worms. Figures 14&15 show data collected through a series of experiments where cDNA of *mig-10* isoforms A and B were tested for their rescue ability. These data show that *mig-10A* and *mig-10B* expressed alone, as well as together, are sufficient to provide complete cell autonomous rescue of the anterior projection truncation of the EC in *mig-10* mutant worms. Furthermore, these data show that cell autonomous expression of *mig-10* isoforms, alone and together, is insufficient to provide full

rescue of posterior projection truncation of the EC. Rather, cell autonomous expression of *mig-10* isoforms provide a wide range of partial rescue to truncation of the posterior projection.

These data show that *mig-10* isoforms are sufficient to provide cell autonomous rescue to anterior projection truncation but are only sufficient at providing partial rescue to posterior projection truncation. This suggests that the mechanism to which MIG-10 contributes varies between anterior and posterior growth. With anterior growth being substantially shorter than posterior growth, it is possible that the anterior mechanism is also much simpler, in the sense that it only requires cell autonomous expression of MIG-10. With a longer growth, such as in the posterior projection, many more guidance cues may be required to assure proper growth. Cues can come from protein gradients present through the length of the worm or they can come from interactions with surrounding cells. In wild type *C. elegans*, MIG-10 is expressed in many different cell types. It is possible that, by mutating *mig-10*, we have also affected the ability of these cells to interact with and guide the posterior projection of the EC. This would account for the inability for *mig-10* isoforms to cell autonomously rescue the posterior projection fully. In future experiments, cell autonomously expressing *mig-10* isoforms in the EC as well as surrounding cells will help to better understand the role of surrounding cells in posterior EC growth as well as the variety of uses of MIG-10 in *C. elegans*.

Our results are inconsistent with previous experiments where fosmids were used to deliver isoforms of *mig-10*. These experiments showed that *mig-10* isoforms, when expressed individually as well as in the same pattern as endogenous MIG-10, were insufficient in providing rescue to the anterior truncation of the EC (Zhang, 2010). Through our results, we have shown that isoforms of *mig-10* are sufficient at providing full rescue of the anterior truncation of the EC when expressed cell autonomously (Figures 14&15). Though these two findings are inconsistent, the two experiments were not controlled for the amount of construct, either fosmid or cDNA, that was introduced into the *mig-10* mutant background. With overexpression, resulting from increased amounts of construct used, the rescue may become greater. Further experiments, controlling for the amount of construct used, can help to test whether these past experiments showed no rescue due to lack of expression or because there is actually no rescue.

Through our experiments, we aimed to examine the role of MIG-10 in EC outgrowth, determine if UNC-53 and MIG-10 work in overlapping pathways, as well as assess the ability of *mig-10* isoforms to cell autonomously rescue *mig-10* mutant defects. By examining embryonic and larval EC growth, we have found that MIG-10 plays a role in embryonic EC development. We have also found that MIG-10 functions differently in the anterior and posterior outgrowths of

the EC. The pathways of MIG-10 and UNC-53 were then examined through the use of single and double mutants. We show that, MIG-10 and UNC-53 interact in different ways depending on the cell being considered. Lastly, with the use of cDNA constructs, we show that *mig-10* isoforms have the ability, both individually as well as together, to provide full cell autonomous rescue to anterior truncation and partial cell autonomous rescue to posterior truncation of the EC in *mig-10* mutant animals. This MQP has shown the complexity in which MIG-10 functions, as well as how it interacts with UNC-53. With the use of our data and past research, we have suggested additional studies which we feel will help lead to a better understanding of the function and pathway of MIG-10 as well as its interaction with UNC-53.

Appendix

MIG-10A Statistical Analysis

Anterior Migration of the Excretory Canal

Between-Subjects Factors

		Value Label	N
Genotype	0	Wild Type	40
	1	mig-10	36
	2	mig-10A Array	30
	3	Array Lost	30

Tests of Between-Subjects Effects

Dependent Variable:Ant.Projection

Source	Type III Sum of Squares	df	Mean Square	F	Sig.
Corrected Model	4.518[a]	3	1.506	120.384	.000
Intercept	26.798	1	26.798	2141.876	.000
Genotype	4.518	3	1.506	120.384	.000
Error	1.651	132	.013		
Total	34.208	136			
Corrected Total	6.170	135			

a. R Squared = .732 (Adjusted R Squared = .726)

Ant.Projection

Tukey HSD[a,,b,,c]

Genotype	N	Subset 1	Subset 2
Array Lost	30	.2520	
mig-10	36	.2790	
mig-10A Array	30		.6176
Wild Type	40		.6404
Sig.		.756	.840

Means for groups in homogeneous subsets are displayed.
Based on observed means.
The error term is Mean Square(Error) = .013.

a. Uses Harmonic Mean Sample Size = 33.488.

b. The group sizes are unequal. The harmonic mean of the group sizes is used. Type I error levels are not guaranteed.

c. Alpha = 0.05.

Multiple Comparisons

Ant.Projection
Tukey HSD

(I) Genotype	(J) Genotype	Mean Difference (I-J)	Std. Error	Sig.	95% Confidence Interval	
					Lower Bound	Upper Bound
Wild Type	mig-10	.3613*	.02570	.000	.2945	.4282
	mig-10A Array	.0227	.02702	.835	-.0476	.0930
	Array Lost	.3883*	.02702	.000	.3180	.4586
mig-10	Wild Type	-.3613*	.02570	.000	-.4282	-.2945
	mig-10A Array	-.3386*	.02765	.000	-.4106	-.2667
	Array Lost	.0270	.02765	.763	-.0449	.0990
mig-10A Array	Wild Type	-.0227	.02702	.835	-.0930	.0476
	mig-10	.3386*	.02765	.000	.2667	.4106
	Array Lost	.3656*	.02888	.000	.2905	.4408
Array Lost	Wild Type	-.3883*	.02702	.000	-.4586	-.3180
	mig-10	-.0270	.02765	.763	-.0990	.0449
	mig-10A Array	-.3656*	.02888	.000	-.4408	-.2905

Based on observed means.
The error term is Mean Square(Error) = .013.

*. The mean difference is significant at the 0.05 level.

Posterior Migration of the Excretory Canal

Between-Subjects Factors

		Value Label	N
Genotype	0	Wild Type	40
	1	mig-10	36
	2	mig-10A Array	30
	3	Array Lost	30

Tests of Between-Subjects Effects

Dependent Variable:Post.Projection

Source	Type III Sum of Squares	df	Mean Square	F	Sig.
Corrected Model	9.303[a]	3	3.101	274.098	.000
Intercept	24.161	1	24.161	2135.631	.000
Genotype	9.303	3	3.101	274.098	.000
Error	1.493	132	.011		
Total	37.493	136			
Corrected Total	10.796	135			

a. R Squared = .862 (Adjusted R Squared = .859)

Post.Projection

Tukey HSD[a,,b,,c]

Genotype	N	Subset 1	Subset 2	Subset 3
mig-10	36	.1992		
Array Lost	30	.2029		
mig-10A Array	30		.4870	
Wild Type	40			.8096
Sig.		.999	1.000	1.000

Means for groups in homogeneous subsets are displayed.
Based on observed means.
The error term is Mean Square(Error) = .011.

a. Uses Harmonic Mean Sample Size = 33.488.

b. The group sizes are unequal. The harmonic mean of the group sizes is used. Type I error levels are not guaranteed.

c. Alpha = 0.05.

Multiple Comparisons

Post.Projection
Tukey HSD

(I) Genotype	(J) Genotype	Mean Difference (I-J)	Std. Error	Sig.	95% Confidence Interval Lower Bound	95% Confidence Interval Upper Bound
Wild Type	mig-10	.6104*	.02444	.000	.5468	.6740
	mig-10A Array	.3227*	.02569	.000	.2558	.3895
	Array Lost	.6067*	.02569	.000	.5399	.6736
mig-10	Wild Type	-.6104*	.02444	.000	-.6740	-.5468
	mig-10A Array	-.2877*	.02629	.000	-.3561	-.2193
	Array Lost	-.0037	.02629	.999	-.0721	.0647
mig-10A Array	Wild Type	-.3227*	.02569	.000	-.3895	-.2558
	mig-10	.2877*	.02629	.000	.2193	.3561
	Array Lost	.2840*	.02746	.000	.2126	.3555
Array Lost	Wild Type	-.6067*	.02569	.000	-.6736	-.5399
	mig-10	.0037	.02629	.999	-.0647	.0721
	mig-10A Array	-.2840*	.02746	.000	-.3555	-.2126

Based on observed means.
The error term is Mean Square(Error) = .011.

*. The mean difference is significant at the 0.05 level.

MIG-10B Statistical Analysis

Anterior Migration of the Excretory Canal

Between-Subjects Factors

		Value Label	N
Genotype	0	Wild Type	40
	1	mig-10	36
	2	mig-10B array	30
	3	array lost	30

Tests of Between-Subjects Effects

Dependent Variable:AnteriorProjection

Source	Type III Sum of Squares	df	Mean Square	F	Sig.
Corrected Model	4.734[a]	3	1.578	177.083	.000
Intercept	26.076	1	26.076	2926.049	.000
Genotype	4.734	3	1.578	177.083	.000
Error	1.176	132	.009		
Total	33.292	136			
Corrected Total	5.911	135			

a. R Squared = .801 (Adjusted R Squared = .796)

AnteriorProjection

Tukey HSD[a,,b,,c]

Genotype	N	Subset 1	Subset 2
array lost	30	.2317	
mig-10	36	.2790	
mig-10B array	30		.6137
Wild Type	40		.6404
Sig.		.175	.655

Means for groups in homogeneous subsets are displayed.
Based on observed means.
The error term is Mean Square(Error) = .009.

a. Uses Harmonic Mean Sample Size = 33.488.

b. The group sizes are unequal. The harmonic mean of the group sizes is used. Type I error levels are not guaranteed.

c. Alpha = 0.05.

Multiple Comparisons

AnteriorProjection
Tukey HSD

(I) Genotype	(J) Genotype	Mean Difference (I-J)	Std. Error	Sig.	95% Confidence Interval	
					Lower Bound	Upper Bound
Wild Type	mig-10	.3613*	.02169	.000	.3049	.4178
	mig-10B array	.0267	.02280	.646	-.0326	.0860
	array lost	.4086*	.02280	.000	.3493	.4680
mig-10	Wild Type	-.3613*	.02169	.000	-.4178	-.3049
	mig-10B array	-.3346*	.02334	.000	-.3954	-.2739
	array lost	.0473	.02334	.183	-.0134	.1080
mig-10B array	Wild Type	-.0267	.02280	.646	-.0860	.0326
	mig-10	.3346*	.02334	.000	.2739	.3954
	array lost	.3819*	.02437	.000	.3185	.4454
array lost	Wild Type	-.4086*	.02280	.000	-.4680	-.3493
	mig-10	-.0473	.02334	.183	-.1080	.0134
	mig-10B array	-.3819*	.02437	.000	-.4454	-.3185

Based on observed means.
The error term is Mean Square(Error) = .009.

*. The mean difference is significant at the 0.05 level.

Posterior Migration of the Excretory Canal

Between-Subjects Factors

		Value Label	N
Genotype	0	Wild Type	40
	1	mig-10	36
	2	mig-10B array	30
	3	array lost	30

Tests of Between-Subjects Effects

Dependent Variable:PosteriorProjection

Source	Type III Sum of Squares	df	Mean Square	F	Sig.
Corrected Model	9.819[a]	3	3.273	409.274	.000
Intercept	24.783	1	24.783	3099.024	.000
Genotype	9.819	3	3.273	409.274	.000
Error	1.056	132	.008		
Total	38.152	136			
Corrected Total	10.875	135			

a. R Squared = .903 (Adjusted R Squared = .901)

PosteriorProjection

Tukey HSD[a,b,c]

Genotype	N	Subset 1	Subset 2	Subset 3
array lost	30	.1802		
mig-10	36	.1992		
mig-10B array	30		.5314	
Wild Type	40			.8096
Sig.		.820	1.000	1.000

Means for groups in homogeneous subsets are displayed.
Based on observed means.
The error term is Mean Square(Error) = .008.

a. Uses Harmonic Mean Sample Size = 33.488.

b. The group sizes are unequal. The harmonic mean of the group sizes is used. Type I error levels are not guaranteed.

c. Alpha = 0.05.

Multiple Comparisons

PosteriorProjection
Tukey HSD

(I) Genotype	(J) Genotype	Mean Difference (I-J)	Std. Error	Sig.	95% Confidence Interval Lower Bound	95% Confidence Interval Upper Bound
Wild Type	mig-10	.6104*	.02054	.000	.5569	.6638
	mig-10B array	.2782*	.02160	.000	.2220	.3344
	array lost	.6294*	.02160	.000	.5732	.6856
mig-10	Wild Type	-.6104*	.02054	.000	-.6638	-.5569
	mig-10B array	-.3322*	.02211	.000	-.3897	-.2747
	array lost	.0190	.02211	.825	-.0385	.0766
mig-10B array	Wild Type	-.2782*	.02160	.000	-.3344	-.2220
	mig-10	.3322*	.02211	.000	.2747	.3897
	array lost	.3512*	.02309	.000	.2911	.4113
array lost	Wild Type	-.6294*	.02160	.000	-.6856	-.5732
	mig-10	-.0190	.02211	.825	-.0766	.0385
	mig-10B array	-.3512*	.02309	.000	-.4113	-.2911

Based on observed means.
The error term is Mean Square(Error) = .008.

*. The mean difference is significant at the 0.05 level.

References

Brenner, S. (May 1974). The Genetics of *Caenorhabditis elegans*. *Genetics* 77: 71–94.

Buechner, M. (2002). Tubes and the single *C. elegans* excretory cell . *Trends in Cell Biology, 12*(10), 479-484.

Chang, C., Adler, C. E., Krause, M., Clark, S. G., Gertler, F. B., Tessier-Lavigne, M., Bargmann, C. I.. (2006). MIG-10/Lamellipodin and AGE-1/PI3K Promote Axon Guidance and Outgrowth in Response to Slit and Netrin. *Current Biology* 16, 854-862

Chilton, J. K. (2006). Molecular mechanisms of axon guidance. *Developmental Biology, 292*(1), 13-24.

Dickson, B. J. (2002). Molecular mechanisms of axon guidance. *Science, 298*(5600), 1959-1964.

Disanza, A., Steffen, A., Hertzog, M., Frittoli, E., Rottner, K., & Scita, G. (2005). Actin Polymerization Machinery: The Finish Line of Signaling Networks, the Starting Point of Cellular Movement. *Cellular and Molecular Life Sciences*, 955-970.

Dubuke, M. and Grant, C. (2009). Abi-1 Interacts with Mig-10, protein interaction in neuronal migration in Caenorhabditis elegans. Major Qualifying Project.

Gosselin, J., and O'Toole, S. (2008). MIG-10, an Adapter Protein, Interacts with ABI-1, a Component of Actin Polymerization Machinery. Major Qualifying Project.

Harrison, M. M., Ceol, C. J., Lu, X., Horvitz, H. R. (2006). Some C. elegans class B synthetic multivulva proteins encode a conserved LIN-35 Rb-containing complex distinct from a NuRD-like complex. *PNAS*. 16782-16787.

Hedgecock, E. M., Culotti, J. G., Hall, D. H., & Stern, B. D. (1987). Genetics of cell and axon migrations in caenorhabditis elegans. *Development (Cambridge, England), 100*(3), 365-382.

Hekimi, S. and Kershaw, D. (1993) Axonal guidance defects in a Caenorhabditis elegans mutant reveal cell-extrinsic determinants of neuronal morphology. *Journal of Neuroscience*. 13(10): 4254-4271

Hobert, O., 2005. Specification of the nervous system. *WormBook*, ed. The *C. elegans* Research Community, WormBook, http://www.wormbook.org.

Jessell, T.M. (200). Neuronal specification in the spinal cord: inductive signals and transcriptional codes. *Nat. Rev., Genet.* 1, 20-29.

Killeen, M. T., & Sybingco, S. S. (2008). Netrin, slit and wnt receptors allow axons to choose the axis of
migration. *Developmental Biology, 323*(2), 143-151.

Kukla, J. (2009). Characterization of the *mig-10(mp0920)* mutant and its effects on migration in *Caenorhabditis elegans*. Major Qualifying Project.

Manser, J., & Wood, W. B. (1990). Mutations affecting embryonic cell migrations in caenorhabditis elegans. *Developmental Genetics, 11*(1), 49-64.

Manser, J., Roonprapunt, C., & Margolis, B. (1997). C. elegans Cell migration gene mig-10Shares similarities with a family of SH2 domain proteins and acts cell nonautonomously in excretory canal development. *Developmental Biology, 184*(1), 150-164.

McDonel, P., Costello, I., Hendrich, B. (2008). Keeping things quiet: Roles of NuRD and Sin3 co-repressor complexes during mammalian development. *Elsevier*. 108-116.

O'Donnell, M., Chance, R. K., & Bashaw, G. J. (2009). Axon growth and guidance: Receptor regulation and signal transduction. *Annual Review of Neuroscience, 32*, 383-412.

Patel, B. N., & Van Vactor, D. L. (2002). Axon guidance: The cytoplasmic tail. *Current Opinion in Cell Biology,14*(2), 221-229.

Quinn, C. C., & Wadsworth, W. G. (2008). Axon guidance: Asymmetric signaling orients polarized outgrowth. *Trends in Cell Biology, 18*(12), 597-603.

Quinn, C. C., Pfeil, S. D., Chen, E., Stovall, L. E., Harden, V. M., Gavin, K. M., Forrester, C. W., Ryder, F. E., Soto, C. M. and Wadsworth, G. W. (2006) UNC-6/Netrin and SLT-1/Slit Guidance Cues Orient Axon Outgrowth Mediated by MIG-10/RIAM/Lamellipodin. *Current Biology*. 16, 845-853.

Schmidt, K. L., Marcus-Gueret, N., Adeleye, A., Webber, J., Baillie, D., Stringham, E. G. (2008) The cell migration molecule UNC-53/NAV2 is linked to the ARP2/3 complex by ABI-1. *Research Article.* 563-573.

Silhankova, M., Korswagen, H. C. (2007) Migration of neuronal cells along the anterior-posterior body axis of C. elegans: Wnts are in control. *Elsevier*. 320-325.

Stringham, E., Pujol, N., Vandekerckhove, J., and Bogaert, T. (2002) *Unc-53* controls longitudinal migration in *C.elegans* development. 3367-3379.

Sulston, J.E., Schrienberg, E., White, J.G., Thomson, J.N. (1983) The Embryonic Cell Lineages of the Nematode *Caenorhabditis elegans*. *Developmental Biology*. 100, 64-119.

Sulston, J.E., & Horvitz, H.R. (1977) Post-embryonic cell lineages of the Nematode, *Caenorhabditis elegans*. *Developmental Biology*. 56, 110-156.

Tessier-Lavigne, M., & Goodman, C. S. (1996). The molecular biology of axon guidance. *Science (New York,N.Y.), 274*(5290), 1123-1133.

Vicente-Manzanares, M., Webb, D., & Horwitz, A. (2005) Cell Migration at a glance. Journal of Cell Science. 118: 4917-4919.

White, J.G., Southgate, E., Thomson, J.N., et al. (1983) Factors That Determine Connectivity in the Nervous System of *Caenorhabditis elegans*. *Cold Spring Harbor Symposia on Quantitative Biology*. 48, 633-640.

Wightman, B., Clark, S.G., Taskar, A.M., Forrester, W.C., Maricq, A.V., Bargmann, C.I., & Garriga G. (1996) The *C. elegans* gene vab-8 guides posteriorly directed axon outgrowth and cell migration. *Development*. 122, 671-682.

Yaron, A., & Zheng, B. (2007). Navigating their way to the clinic: Emerging roles for axon guidance molecules in neurological disorders and injury. *Developmental Neurobiology, 67*(9), 1216-1231.

Yoshikawa, S. & Thomas, J.B. (2004). Secreted cell signaling molecules in axon guidance. *Current Opinion in Neurobiology.* 14, 45-50.

Yu, T. W., & Bargmann, C. I., (2001). Dynamic regulation of axon guidance. *Nature Neuroscience, 4*(11),
1169.

Zhang, S. (2010). Functional analysis of MIG-10: a cytoplasmic adaptor protein important in neuronal migration and process outgrowth in C. elegans. Major Qualifying Project.